

# THE USE OF FINITE ELEMENT-DERIVED SHAPE FUNCTIONS TO SIMPLIFY THE MODELING OF STRUCTURAL COMPLIANCE IN ADAMS

## ABSTRACT

The incorporation of discretely-idealized structures directly into MSS models can lead to a considerable increase in analytical model size with a subsequent, undesirable growth in problem complexity and solution time. Under conditions where the foundation structure mass effects are secondary and the structural deformations of interest are orthogonal and uncoupled spatially, the use of shape functions derived from finite element analysis offers a substantial simplification of the problem. The technique is illustrated by the analysis of the rolling contact forces associated with a multiple-wheeled carriage rolling along an elastic foundation. The application of the method to a steel mill bridge crane transporting steel ladles is discussed.

The modeling of continuous, moving contact in Mechanical System Simulation (MSS) is, in general, relatively simple as long as the contact path is smooth, continuous, and either perfectly rigid or subject to simple, position-independent flexibility. An example of the former might be a bead sliding along a rigid curvilinear path under the influence of gravity. This type of motion is rather easily achieved in ADAMS [1] with the point-to-curve (PTCV) or curve-to-curve (CVCV) constraint utilities. An example of the second type mentioned, e.g., position-independent flexibility, occurs when the contact flexibilities are spatially independent of the contact location. An SFORCE model of a ball bouncing along the ground is an example of this. A more sophisticated example might be the ADAMS TIRE aggregate element. Even though the tire properties might be complex, they do not depend on where the tire is at any point in time.

Fig. 1 below shows an ADAMS/VIEW [2] image of a single, flexible wheel rolling along a straight rail.

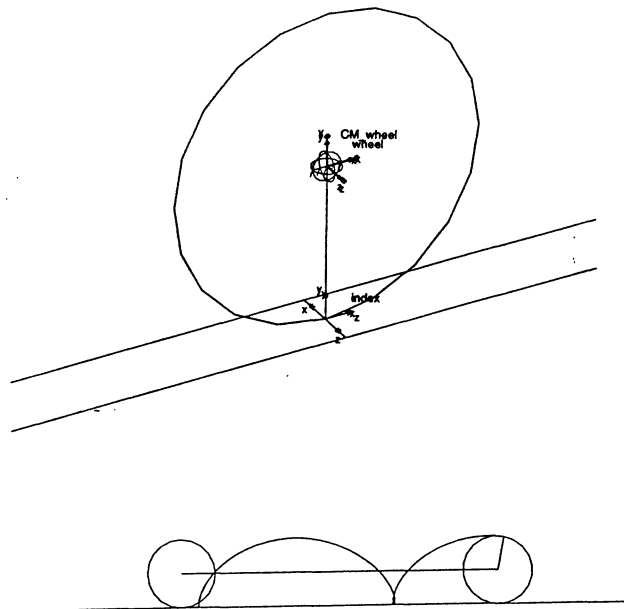


Fig. 1 Sliding/Rolling Motion of GFORCE-Based Wheel

The wheel forces are implemented using an ADAMS GFORCE. Initially, the wheel is given a translational velocity only, so it slips until sliding friction imparts rolling motion to it, after which a point on the rim describes a classical, trochoidal path. The GFORCE expression for the wheel is given below.

```
!
!               adams_view_name='trnww1WF'
GFORCE/17
, I = 216
, JFLOAT = 17
, RM = 49
, FX = 0.2*impact(dy(216,49,49),vy(216,49,49),1.25,1e8,1.1,1e5,.01)
,      *step(vx(216,49,49)+wz(216,49,49)*dy(216,49,49),-.1,+1,+.1,-1)\
, FY = impact(dy(216,49,49),vy(216,49,49),1.25,1e8,1.1,1e5,.01)\
, FZ = -1e8*dz(216,49,49)*step(dy(216,49,49),1.25,1,1.385,0)\
, TX = +1e8*dz(216,49,49)*step(dy(216,49,49),1.25,1,1.385,0)*dy(216,49,49)\
, TY = 0\
, TZ = (0.2*impact(dy(216,49,49),vy(216,49,49),1.25,1e8,1.1,1e5,.01)
,      *step(vx(216,49,49)+wz(216,49,49)*dy(216,49,49),-.1,+1,+.1,-1))
,      *dy(216,49,49)
```

In this expression;

```
wheel center marker ID ----- 216
rail datum marker ID ----- 49
wheel stiffness (lb/ft) ----- 1.0E8
wheel damping (lb-sec/ft) ----- 1.0E5
wheel radius (ft) ----- 1.25
coef. of sliding friction ----- 0.20
deflection @ full damping (ft)----- 0.01
wheel center to rail surface distance
for flange disengagement (ft) ----- 1.385
```

(note: the applied trunnion load is 5.0E6 lb)

The GFORCE employs a linear force-displacement algorithm vertically and laterally. From these forces and a computed slip ratio based on instantaneous translational and rotational velocities, the tractive force, rolling moment, and overturning moments are computed (the aligning moment is assumed zero). When included with other carriage components, the wheel is brought into motion by specifying either a displacement or velocity constraint on the revolute joint attaching the wheel to its bogie (not shown). The contact forces, vertical and lateral are referenced to a marker fixed in the rail surface. Should the wheel lift off the rail, all forces go to zero. The stiffness of the wheel/rail contact is position-independent, and the associated deflection of the wheel will be the same for a given load, regardless of the wheel's position along the rail.

Fig. 2 below traces the trunnion center of a 2-wheeled bogie employing the same algorithm given above as it moves (under exaggerated loading) along a perfectly rigid railway. The motion of the bogie is the result of a time-dependent MOTION statement imposed on one of the wheels. Clearly, the trace shows the independence of the wheel deformation ( $=0.05$  ft) with respect to position along the rail. The loading and stiffnesses are constant, hence the vertical deformation is constant along the path.

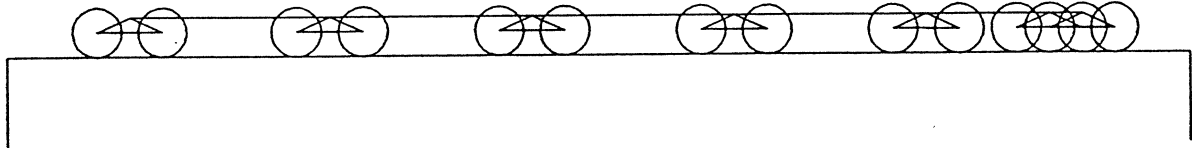


Fig. 2 Wheel Bogie Moving Along Rigid Railway.

Assume now that we wish to include the foundation flexibility of the sub-rail support structure in the analysis. At its simplest, this structure can be discretized into 2 end PARTs, each representing half the total beam mass and inertia. These parts are connected by an ADAMS BEAM with the following properties:

length (ft)	-----	60.0
Inertia (ft <sup>4</sup> )	-----	9.528
Modulus of Elasticity (lb/ft <sup>2</sup> )	-----	4.32E9

For each wheel, TWO GFORCES are now required, one for each beam half. A STEP function whose value varies from 0 to 1 is used to switch between the two gforces based on the wheel's instantaneous position along the rail. The beam position at which the switch takes place is up to the user. One could begin to turn the wheel force on the right beam end off and that on the left end on over, say, a range from 25 to 35 ft from the right beam end. In our case, the 'rise' of the step function covers the entire span. Thus, when a wheel is directly over the right end of the span, the wheel force is distributed 100% to the right beam half and 0% to the left beam half. When the wheel is at the geometric midspan, 50% of its load is applied to the right beam half and 50% to the left beam half, and so on. This method has the disadvantage that the datum markers locating the rigid rail surface for each part always reference the tangent to the elastic axis of the beam at the datum marker location rather than the elastic axis itself and will exaggerate the beam deformation, especially at mid-span. Fig. 3 shows the same bogie previously discussed, now moving along the discrete elastic foundation. It can be seen from the superimposed plots that

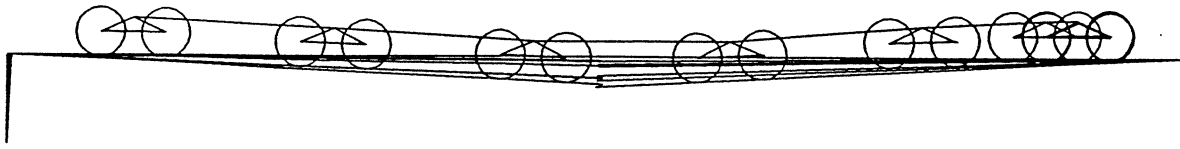


Fig. 3 Wheel Bogie Moving along a (Discrete) Flexible Railway

elastic foundation effects are present, with a maximum trunnion deflection of approximately 1.2 ft at the midspan. A simple check against classical beam theory predicts a deflection of 0.525 ft for this simply-supported beam loaded at midspan (note --the comparison is approximate since the bogie wheels are actually on 32 inch centers). As more and more PARTs and BEAMs are used to discretize the structure, this exaggeration diminishes. Sheppardson [3] and Elliott[4] have shown that extremely precise static and dynamic results can be obtained by this method. However, when continuous contact modeling is required, the number of GFORCES, hence equations, can grow substantially since each wheel in the system must have a GFORCE for each discrete beam part. When modeling high-speed locomotive rail/wheel contact, Hoban and Elliott [5] circumvented the inaccuracies associated with using displacement references tangential to the end of the elastic axis by employing mathematically-derived shape functions (in this case, Hermitian polynomials) to represent the rail deflection between the roadbed ties, which were themselves elastically sprung to ground. Because the rail/tie mass effects were important, the wheel forces still had to be transferred from span-to-span, requiring complex FORTRAN subroutines and a large ADAMS model.

In the initial stages of modeling a steel mill bridge crane system, thought was given to using the previously-cited method. The large projected model size, combined with the intrinsic irregularities of the building rail support structure mitigated against discretizing the flexible structures. Further, mass considerations were considered limited to the crane components themselves. Thus, as an alternative, it was decided to examine the possibility of including foundation compliance effects through modifying the wheel stiffnesses by altering their elastic properties based on the instantaneous positions and loadings of all the wheels contacting the rail span.

For a simple systems in which the wheel is elastic and the rail rigid, the force-deflection relationship is given by;

$$\text{Eq. 1)} \quad \{F_w\} = [K_w]\{\delta_w\}$$

where;  $\{F_w\}$  = wheel system force vector,  
 $[K_w]$  = wheel system stiffness matrix,  
 $\{\delta_w\}$  = wheel system deflection vector.

The stiffness matrix  $[K_w]$  is diagonal, each term representing the (independent) contact stiffness of its respective wheel. If the wheels are identical, each term will be identical and eqn.1 can be written as;

$$\text{Eq. 2)} \quad \{F_w\} = \kappa_w[I]\{\delta_w\}$$

where;  $\kappa_w$  = the (scalar) value of the common wheel stiffness.

Assume now that the foundation is capable of yielding under the presence of forces acting on it. A load **anywhere** on the span will result in a deflection **everywhere** along the span, excepting, of course, at grounded supports. By applying successive, unit loads at the instantaneous wheel positions along the span, multiplying these loads by the actual instantaneous wheel load, and measuring the resulting deflection at all selected points along the span, a dynamic 'influence coefficient' matrix  $[G_r]$  is created. The (global) deflection at any wheel will now include a component due to the all the wheel forces acting on the structure, as;

$$\text{Eq. 3)} \quad \delta_{ci} = \delta_{wi} + \sum_{j=1}^{n_w} G_{rij} \cdot F_{wj}$$

where ;  $\delta_{ci}$  = global (combined) deflection of the ith wheel,  
 $F_{wj}$  = the jth wheel force,  
 $n_w$  = the number of wheels

It should be kept in mind that the influence coefficient matrix used in defining the 'give' of the foundation varies functionally with the (x) position of each wheel in the set. Thus;

$$\text{Eq. 4)} \quad G_{rij} = G_{rij}(x)$$

In matrix form, eqn. 3 becomes;

$$\text{Eq. 5)} \quad \{\delta_c\} = \{\delta_w + [G_r]\{F_w\}\}$$

If the deflection due to the wheel spring is written in influence coefficient form, eqn. 5 becomes;

$$\text{Eq. 6)} \quad \{\delta_c\} = [[G_w] + [G_r]]\{F_w\}$$

Adding the two influence coefficients into a composite coefficient and realizing that any influence coefficient has a corresponding inverse known as the stiffness matrix;

$$\text{Eq. 7)} \quad [G_w] + [G_r] = [G_c] = [K_c]^{-1}$$

The elastic portion of the structural problem can now be written as;

$$\text{Eq. 8)} \quad \{F_w\} = [K_c]\{\delta_c\}$$

The key to the method is to track the instantaneous positions of the wheels and, by some means, modify the effective stiffnesses of the wheels as a function of these positions. This is accomplished by using FEA to 'map' the structure at (fixed) discrete points over its span and encoding this data in an ADAMS SPLINE function which can interpolate the position-dependent, instantaneous stiffnesses from the fixed-point data. Fig. 4 shows a NASTRAN [6] model of a (simply-supported) crane beam. The rail surface is at the top of the beam and is represented by a series

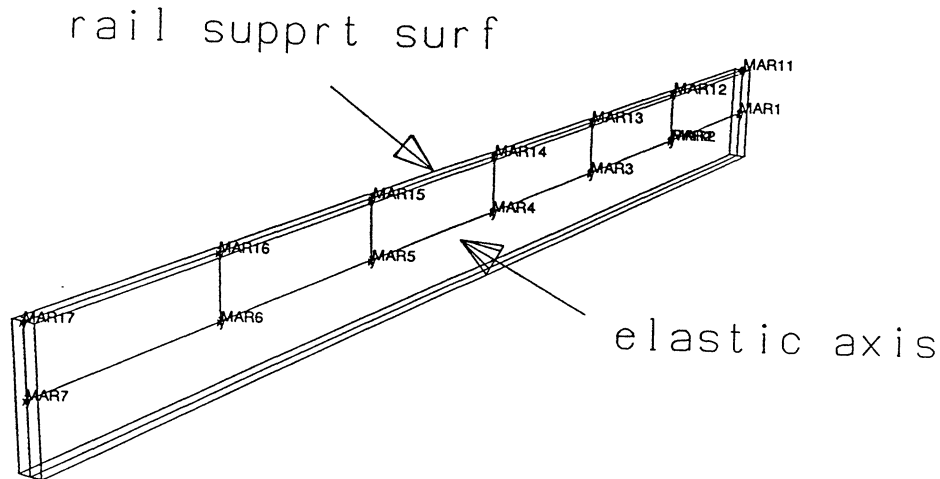


Fig. 4 NASTRAN Model of Bridge Crane Transverse Beam

of GRIDs projected up on stiff (essentially rigid) extensions from the beam elastic axis. While not effecting the vertical deformations of the beam, it is important that the 'rolling' surface be properly located for correct lateral deflections since the torsional deformation, acting over the distance from the beam neutral axis to this surface will, in general, contribute significantly to the rail lateral deflections.

For each applied load, the deformations in the loaded direction are extracted and written in the form of an ADAMS SPLINE. The spline can be interpreted by reading across the spline for loading position and down the spline for deformation position (or vice versa since, like a global stiffness matrix, an influence coefficient is positive semidefinite, hence symmetric).

```

!               adams_view_name='bridge_flexv'
!               adams_view_units='no_units'
SPLINE/6
, X = -15, 0, 15, 30, 45, 60, 75
, Y = -15, 1.36E-07, 0, -7.17E-08, -8.19E-08, -5.12E-08, 0, 5.46E-08
, Y = 0, 0, 0, 0, 0, 0, 0, 0
, Y = 15, -7.17E-08, 0, 6.15E-08, 7.51E-08, 4.78E-08, 0, -5.12E-08
, Y = 30, -8.19E-08, 0, 7.51E-08, 1.09E-07, 7.51E-08, 0, -8.19E-08
, Y = 45, -5.12E-08, 0, 4.78E-08, 7.51E-08, 6.15E-08, 0, -7.17E-08
, Y = 60, 0, 0, 0, 0, 0, 0, 0
, Y = 75, 5.46E-08, 0, -5.12E-08, -8.19E-08, -7.17E-08, 0, 1.36E-07
!
!               adams_view_name='bridge_flexl'
!               adams_view_units='no_units'
SPLINE/7
, X = -15, 0, 15, 30, 45, 60, 75
, Y = -15, 1.67E-06, 0, -7.81E-07, -8.92E-07, -5.58E-07, 0, 5.95E-07
, Y = 0, 0, 0, 0, 0, 0, 0, 0
, Y = 15, -7.81E-07, 0, 8.08E-07, 9.1E-07, 5.67E-07, 0, -5.58E-07
, Y = 30, -8.92E-07, 0, 9.1E-07, 1.37E-06, 9.1E-07, 0, -8.92E-07
, Y = 45, -5.58E-07, 0, 5.67E-07, 9.1E-07, 8.08E-07, 0, -7.81E-07
, Y = 60, 0, 0, 0, 0, 0, 0, 0
, Y = 75, 5.95E-07, 0, -5.58E-07, -8.92E-07, -7.81E-07, 0, 1.67E-06
!

```

Note that, although the beam length is 60 ft, a 15 ft 'over-run length has been added to each end beyond the supports. A force expression which accesses the spline is shown below. This expression is functionally identical to the algorithm given for the single wheel on a rigid rail except that ADAMS VARIABLE expressions are now used to modify the displacement datums (DYs and DZs) used to determine the wheel forces. The use of the VARIABLE expression is not strictly necessary, but the GFORCE expressions tend to become rather large and unwieldy without them.

```

!
!               adams_view_name='trnww1WF_VAR1'
!
VARIABLE/171,IC=0.0,
, FUN=DY(216,49,49)
,-GFORCE(17,0,3,49)*(-1.0)*
, AKISPL(DZ(216,46,46),
, DZ(216,46,46),6)
,-GFORCE(18,0,3,49)*(-1.0)*
, AKISPL(DZ(217,46,46),
, DZ(216,46,46),6)
!
!               adams_view_name='trnww1WF_VAR2'
!
VARIABLE/172,IC=0.0,
, FUN=DZ(216,49,49)
,-GFORCE(17,0,4,49)*(-1.0)*
, AKISPL(DZ(216,46,46),
, DZ(216,46,46),7)
,-GFORCE(18,0,4,49)*(-1.0)*
, AKISPL(DZ(217,46,46),
, DZ(216,46,46),7)
!               adams_view_name='trnww1WF'
GFORCE/17
, I = 216
, JFLOAT = 17

```

```

, RM = 49
, FX = 0.2*IMPACT(VARVAL(171),VY(216,49,49),1.25,1E8,1.1,1E5,.01)
,   *STEP(VX(216,49,49)+WZ(216,49,49)*VARVAL(171),-.1,+1,.1,-1)\
, FY = -1E8*(VARVAL(171)-1.25)-1E5*VY(216,49,49)\
, FZ = -1E8*(VARVAL(172))*STEP(VARVAL(171),1.25,1,1.385,0)\
, TX = +1E8*VARVAL(172)*STEP(VARVAL(171),1.25,1,1.385,0)
,   *VARVAL(171)\
, TY = 0\
, TZ = (0.2*IMPACT(VARVAL(171),VY(216,49,49),1.25,1E8,1.1,1E5,.01)
,   *STEP(VX(216,49,49)+WZ(216,49,49)*VARVAL(171),-.1,+1,.1,-1))
,   *VARVAL(171)

```

In passing it should be noted that the AKISPLINE function will use cubic interpolation along the abscissal values, and linear interpolation between the ordinate curves. Also, the tacit assumption has been made all along that the structural deformations are linear, an assumption which is implicit in the FEA model.

Fig. 5 shows the path of the bogie trunnion as it moves along the simply-supported beam, the flexibility of which is now represented using interpolated shape functions.

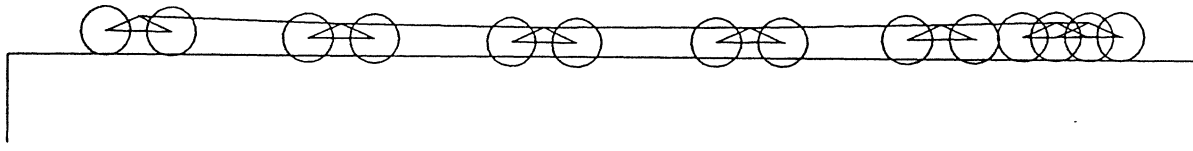
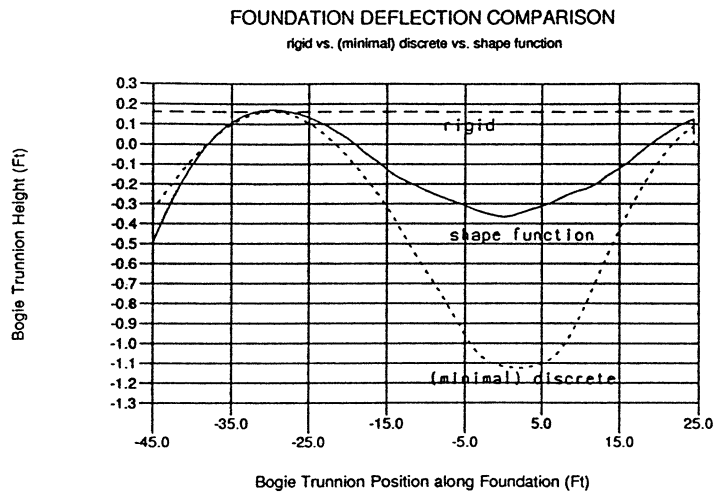


Fig. 5 Bogie Moving on Shape-function Defined Flexible Foundation

The changes in the foundation stiffness as the bogie traverses the structure are clearly evident. Fig. 6 plots the bogie trunnion vertical position as a function of trunnion position along the beam for the three different models discussed. The vertical deflection for the model employing the





- Fig. 6 Comparison of Trunnion Deflections

shape functions is about .545ft. This is slightly more than classical theory would predict, but it includes the effects of wheel flexibility, which are about one order of magnitude less than the beam flexibility itself.

Fig. 7 shows an ADAMS/VIEW image of a model of a steel mill bridge crane used to transfer ladles of molten steel in a 'teeming aisle' during processing. NASTRAN models of the

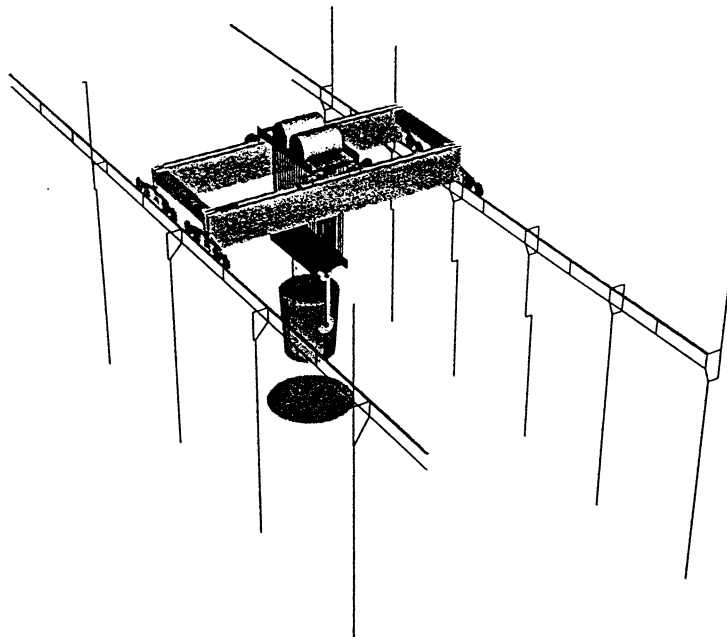


Fig. 7 Steel Mill Bridge Crane Model

building structure have been used to generate influence coefficient splines for the aisle girderways in the same fashion as described for the simply-supported beam detailed earlier. Compared with the bridge beam, the nature of the building structure is highly irregular but still sufficiently 'cellular' that the railway horizontal and vertical deflections can be considered uncoupled. Fig. 8 gives a plot of an exaggerated system event in which the bridge is moved at maximum speed along the girderway (to the west) while the ladle trolley is run up to full speed

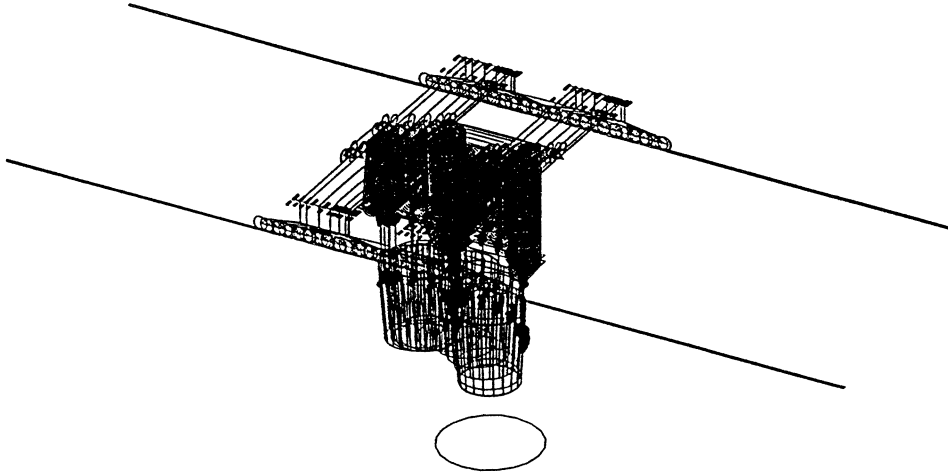


Fig. 8 Hypothetical Bridge Crane Operational Cycle

along the bridge (to the north) and then subjected to maximum braking. Fig 9 compares the total north girder reactions for a model in which bridge and girderway flexibility has been ignored to

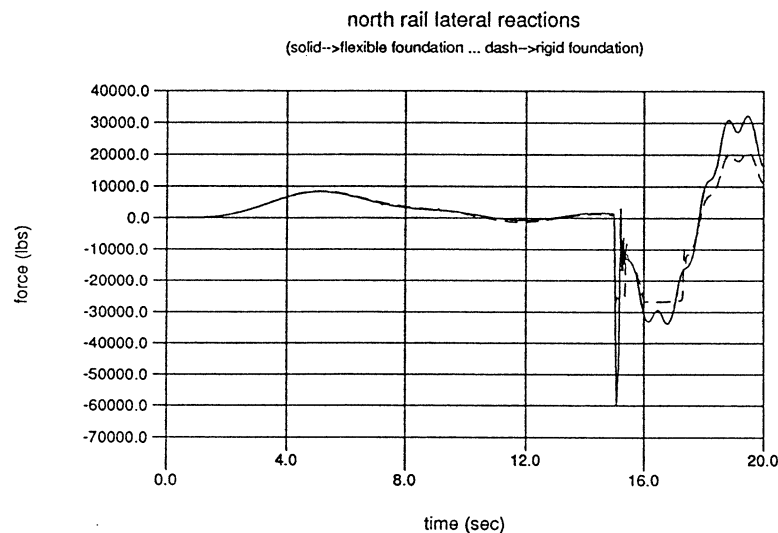


Fig 9 Girderway Reactions -- Flexible vs. Rigid Foundations

one in which the vertical and lateral flexibility has been included. As can be seen, the inclusion of elastic effects has resulted in a substantial change to, both, the peak load level and the number of loading excursions. These changes may be very significant when attempting to satisfy building codes. Doubly so since, when specific, dynamic structural analysis is not available, **very** conservative static load factors are often mandated by current building codes.

## DISCUSSION

The use of FEA-derived shape functions within ADAMS analyses of systems involving elastic foundation phenomena appears viable and useful. The method offers the following limitations and advantages:

#### Limitations:

- 1) method limited to small displacements
- 2) Foundation mass effects are ignored
- 3) Process requires significant manual data transfer

#### Advantages:

- 1) The model is substantially reduced in size
- 2) Contact phenomena are guaranteed to be numerically 'smooth' due to use of splines
- 3) Solution times are comparable to those for non-flexible models.

The limitations cited above may prove surmountable with additional effort. Large displacement effects may be achievable with more complex foundation force expressions capable of representing material nonlinearity as well as the geometric cross-coupling associated with large displacement effects. It would appear that shape functions might also be used to include mass effects. The wheel force expressions would then contain acceleration-dependent terms acting on spline-determined mass properties. This may prove a subject for further study.

### References

- 1) ADAMS/Solver Reference Manual Version 7.0, anon, Oct. 7/93 Mechanical Dynamics, Inc. Ann Arbor, MI
- 2) ADAMS/View User's Reference Manual Version 7.0, anon, Oct. 7/93 Mechanical Dynamics, Inc. Ann Arbor, MI
- 3) Representation of Component Flexibility in Multibody Dynamics through Component Discretization, Sheppardson, K. C., (Masters Thesis), U. of M. 1990
- 4) Application of a General-Purpose Mechanical System Analysis Code to Rotorcraft Dynamics Problems, Elliott, A. S. and J. B. McConville, Proceedings of the National Specialists Meeting on Rotorcraft Dynamics, American Helicopter Society, Southwest Region, Arlington, TX, 1989
- 5) Railroad Bed Modeling Hoban, John, Elliott, A., (Unpublished) Mechanical Dynamics, Inc. Ann Arbor, MI 1992
- 6) NASTRAN Handbook of Linear Analysis, anon, MacNeal-Schwendler, Los Angeles, CA 1985